JCI The Journal of Clinical Investigation

N-acetylcysteine reduces the size and activity of von Willebrand factor in human plasma and mice

Junmei Chen, Adili Reheman, Francisca C. Gushiken, Leticia Nolasco, Xiaoyun Fu, Joel L. Moake, Heyu Ni, José A. López

J Clin Invest. 2011;121(2):593-603. https://doi.org/10.1172/JCI41062.

Research Article

Thrombotic thrombocytopenic purpura (TTP) is a life-threatening disease characterized by systemic microvascular thrombosis caused by adhesion of platelets to ultra-large vWF (ULVWF) multimers. These multimers accumulate because of a deficiency of the processing enzyme *ADAMTS13*. vWF protein forms long multimers from homodimers that first form through C-terminal disulfide bonds and then join through their N termini by further disulfide bonding. N-acetylcysteine (NAC) is an FDA-approved drug that has long been used to treat chronic obstructive lung disease and acetaminophen toxicity and is known to function in the former disorder by reducing mucin multimers. Here, we examined whether NAC could reduce vWF multimers, which polymerize in a manner similar to mucins. In vitro, NAC reduced soluble plasma-type vWF multimers in a concentration-dependent manner and rapidly degraded ULVWF multimer strings extruded from activated ECs. The effect was preceded by reduction of the intrachain disulfide bond encompassing the platelet-binding A1 domain. NAC also inhibited vWF-dependent platelet aggregation and collagen binding. Injection of NAC into *ADAMTS13*-deficient mice led to the rapid resolution of thrombi produced by ionophore treatment of the mesenteric venules and reduced plasma vWF multimers. These results suggest that NAC may be a rapid and effective treatment for patients with TTP.

N-acetylcysteine reduces the size and activity of von Willebrand factor in human plasma and mice

Junmei Chen,[1] Adili Reheman,[2] Francisca C. Gushiken,[3] Leticia Nolasco,[4] Xiaoyun Fu,[1,5] Joel L. Moake,[4] Heyu Ni,[2,6] and José A. López[1,5]

[1]Puget Sound Blood Center, Seattle, Washington, USA. [2]Department of Laboratory Medicine and Pathobiology, St. Michael's Hospital, University of Toronto, Toronto, Ontario, Canada. [3]Baylor College of Medicine, Houston, Texas, USA. [4]Rice University, Houston, Texas, USA. [5]University of Washington, Seattle, Washington, USA. [6]Canadian Blood Services, Toronto, Ontario, Canada.

Thrombotic thrombocytopenic purpura (TTP) is a life-threatening disease characterized by systemic microvascular thrombosis caused by adhesion of platelets to ultra-large vWF (ULVWF) multimers. These multimers accumulate because of a deficiency of the processing enzyme *ADAMTS13*. vWF protein forms long multimers from homodimers that first form through C-terminal disulfide bonds and then join through their N termini by further disulfide bonding. N-acetylcysteine (NAC) is an FDA-approved drug that has long been used to treat chronic obstructive lung disease and acetaminophen toxicity and is known to function in the former disorder by reducing mucin multimers. Here, we examined whether NAC could reduce vWF multimers, which polymerize in a manner similar to mucins. In vitro, NAC reduced soluble plasma-type vWF multimers in a concentration-dependent manner and rapidly degraded ULVWF multimer strings extruded from activated ECs. The effect was preceded by reduction of the intrachain disulfide bond encompassing the platelet-binding A1 domain. NAC also inhibited vWF-dependent platelet aggregation and collagen binding. Injection of NAC into *ADAMTS13*-deficient mice led to the rapid resolution of thrombi produced by ionophore treatment of the mesenteric venules and reduced plasma vWF multimers. These results suggest that NAC may be a rapid and effective treatment for patients with TTP.

Introduction

Thrombotic thrombocytopenic purpura (TTP) is a catastrophic and potentially fatal disorder caused by systemic microvascular thrombosis affecting many organs, including liver, kidneys, heart, pancreas, and brain (1). Early speculation about its pathogenesis suggested the presence of a platelet-aggregating factor in the blood of patients (2). In 1982, Moake et al. (3) noted the presence of unusually large forms of von Willebrand factor (ultra-large vWF [ULVWF]) in patients with chronic TTP in remission and proposed that these molecules were responsible for the clinical manifestations of the disorder. These investigators also posited that ULVWF accumulated because of a deficiency in the activity of a vWF "depolymerase." In the years since that seminal publication, both the suggestion that ULVWF has a causative role in TTP and the speculation of a deficient depolymerase have proven correct. Compared with vWF, ULVWF is hyperfunctional in binding platelets (4), collagen (5), and erythrocytes (6). In addition, accumulation of ULVWF in TTP was indeed found to be caused by congenital or acquired deficiency of a vWF depolymerase, one that produces smaller vWF polymers proteolytically, the metalloprotease *ADAMTS13* (7, 8).

The current standard of care for familial TTP is infusion of fresh-frozen plasma and for acquired TTP is plasma exchange with or without immunosuppressive therapy (9). Plasma infusion provides *ADAMTS13*, which is not produced in the patients with congenital deficiency; plasma exchange removes anti-*ADAMTS13* autoantibodies and replaces *ADAMTS13* unbound to autoantibody. This therapy has proven effective in reducing mortality; however, it requires specialized equipment and nursing available primarily in tertiary medical centers, and it exposes patients to many liters of blood products. Because of the need to mobilize specialized personnel and equipment, treatment may be delayed when the diagnosis is uncertain. Furthermore, some patients with acquired TTP do not respond to plasma exchange.

In this study, we explored a potentially easier treatment for TTP that targets the main culprit in the disorder, ULVWF. This therapy, N-acetylcysteine (NAC), was suggested by the peculiarities of vWF synthesis and processing, and by homology of vWF to polymeric mucins, as illustrated below.

The newly translated pre-pro-vWF polypeptide contains 2813 amino acids and 4 distinct types of domains, A, B, C, and D, arranged as follows from N terminus to C terminus: D1-D2-D′-D3-A1-A2-A3-D4-B1-B2-B3-C1-C2-CK, with D1-D2 comprising the propolypeptide sequence and the mature polypeptide beginning with the D′ domain (10).

During its synthesis, vWF forms extremely long polymers, consisting of dimers (the protomeric units) strung end to end. The dimers form in the endoplasmic reticulum through disulfide bonds between C-terminal cysteines in the CK domains, then polymerize in the *trans*-Golgi compartment by N-terminal disulfide bonds (11).

In overall structure, vWF is strikingly similar to the polymeric mucins, including porcine submaxillary mucin, MUC2, MUC5AC, MUC5B, and MUC6 (12). Like vWF, these mucins have CK domains at the C terminus and D domains at the N terminus, which they use to dimerize in the endoplasmic reticulum and multimerize in the *trans*-Golgi (12).

Mucins are the main protein components of mucus. While normally playing a lubricating role, mucus sometimes become

Conflict of interest: The authors have declared that no conflict of interest exists.
Citation for this article: *J Clin Invest.* 2011;121(2):593–603. doi:10.1172/JCI41062.

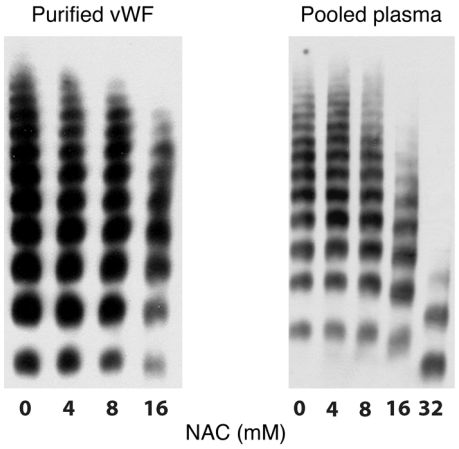

Figure 1
NAC reduces vWF multimers under static conditions. Purified plasma vWF (left) or pooled human plasma (right) were incubated with NAC at 37°C for either 30 minutes (purified vWF) or 1 hour (plasma), at which time the reactions were stopped by the addition of NEM to alkylate the residual NAC. vWF multimers were then examined by electrophoresis on a 1% agarose gel followed by immunoblotting. NAC reduced vWF multimer size in a concentration-dependent manner.

dehydrated and viscous, which in patients with congestive and obstructive lung diseases that include chronic bronchitis and cystic fibrosis can produce serious complications because of their difficulty in clearing it from the airways. One strategy employed for over 50 years to decrease airway congestion and improve ventilation in these disorders has been the use of NAC as a mucolytic agent (13). This simple compound, which comprises L-cysteine with an acetyl moiety attached to the amine group, contains a free thiol and is capable of decreasing mucin size and viscosity by reducing disulfide bonds connecting the mucin monomers (14).

Because of the similarities of vWF and polymeric mucins, we explored the possibility that NAC could also reduce the size and reactivity of ULVWF, potentially as a means of treating TTP. In this report, we describe the effects of NAC on vWF structure and functions both in vitro and in vivo.

Results

We examined whether, by analogy with its effect on polymeric mucins, NAC could reduce the size and reactivity of vWF, using purified human vWF, human plasma, and wild-type and *ADAMTS13*$^{-/-}$ mice. We then examined the effect of this treatment on vWF-related platelet functions in vitro and thrombus formation in vivo.

NAC reduces vWF under static conditions. We first examined the effect of NAC on vWF multimer structure using either purified plasma vWF or pooled human plasma (Figure 1). In both cases, the extent of multimer reduction increased with increasing NAC concentration.

NAC effect on ULVWF strings. These experiments were conducted using a parallel-plate flow chamber, with the floor of the chamber consisting of a 35-mm culture dish coated with endothelial cells. The endothelial cells were stimulated with histamine, and the chamber was then perfused with platelets suspended in buffer at a shear stress of 2.5 dynes/cm^2. When perfused subsequently with platelet-free buffer, the platelet-decorated strings remained stable for at least 5 minutes (Supplemental Video 1; supplemental material available online with this article; doi:10.1172/JCI41062DS1). When perfused with buffer containing NAC (40 mM), however, the strings began to disappear within 2 minutes, and within 5 minutes almost 80% of the strings were gone (Supplemental Video 2 and Figure 2). With NAC, the strings stretched considerably before they detached and embolized downstream, unlike what we have observed with *ADAMTS13* treatment of the strings, when *ADAMTS13* cleaves the strings without prior elongation. At times we observed string fragments from upstream regions of the slide enter the field and transiently associate with existing strings before detaching again and floating downstream. Quantification of string number underestimated the extent to which NAC reduced endothelial surface–associated platelets because even when strings remained on the endothelial surface after NAC perfusion, the quantity of platelets associated with the strings was greatly diminished.

NAC disrupts the disulfide bond in the vWF A1 domain. The stretching of vWF stings before their scission suggests that NAC may be reducing intrachain disulfides before it affects the interchain

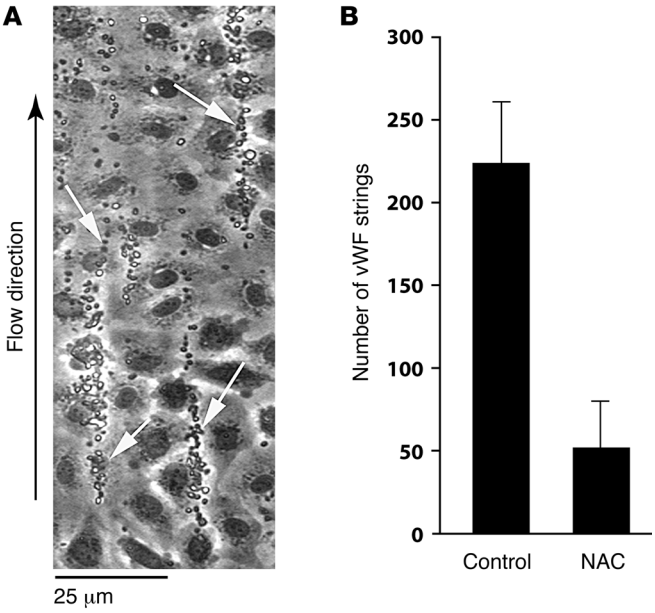

Figure 2
Effect of NAC on platelet–vWF strings under flow. (**A**) Platelets adherent to vWF strings secreted from, and anchored to, histamine-stimulated HUVECs are marked with arrows. (**B**) Quantification of the platelet-vWF strings. The number of platelet-vWF strings after perfusion with 40 mM NAC was 23% of the untreated control ($P < 0.001$). Mean values of string number with SD from 5–9 experiments are shown. The data were analyzed using Student's *t* test.

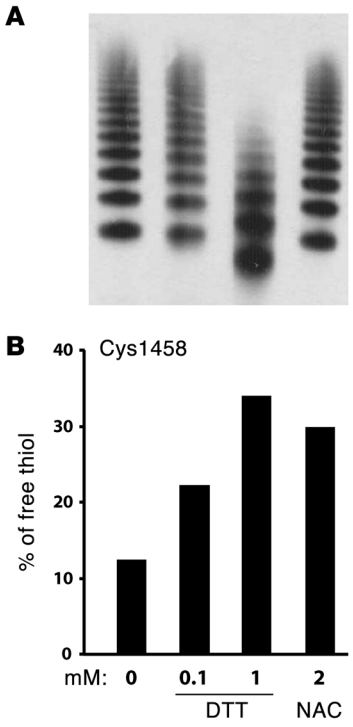

Figure 3
DTT and NAC reduced the Cys1272–Cys1458 disulfide bond in the vWF A1 domain under shear. Purified plasma vWF was sheared on a cone-and-plate viscometer at 37°C, 10,000 s^{-1} for 15 minutes in the presence of 25 mM HEPES buffer (0 mM), DTT, or NAC. The samples were then mixed immediately with NEM to prevent further disulfide bond shuffling. The percentage of Cys1458 in the vWF A1 domain existing as a free thiol was quantified by mass spectrometry. (**A**) vWF multimers were examined by SDS-agarose electrophoresis and immunoblotting with a polyclonal vWF antibody. (**B**) The percentage of Cys1458 existing in the free thiol form increased in the presence of DTT or NAC.

bonds. One disulfide bond of particular interest, Cys1272–Cys1458 in the A1 domain, is required for platelet GPIbα binding (15). We therefore determined whether NAC reduces this bond as another means of decreasing vWF reactivity. We used mass spectrometry to detect free thiols in purified plasma vWF multimers treated with either NAC or another reducing agent, dithiothreitol (DTT). The vWF was first mixed with the reducing agents, sheared in a cone-and-plate viscometer, and then treated with *N*-ethylmaleimide (NEM) to alkylate the free thiols produced. vWF multimer structure was examined using 1 aliquot of each sample, and the remainder was fully reduced under denaturing conditions with DTT. The free thiols exposed under this condition were alkylated with isotope-labeled NEM (NEM-d5), which has a molecular mass 5-mass unit greater than that of NEM. The samples were digested into smaller peptides and the NEM- or NEM-d5–labeled peptides were examined and quantified by mass spectrometry. Under these conditions, NAC (2 mM) increased the percentage of Cys1458 existing in the free thiol form without apparently affecting the multimer pattern (Figure 3). In contrast, 1 mM DTT, with the same free thiol concentration as 2 mM NAC, not only increased the percentage of Cys1458 existing as a free thiol; it also significantly reduced vWF multimer size (Figure 3). These experiments were carried out at a shear rate of 10,000 sec^{-1}, which produces a shear stress approximately equivalent to that found in human arterioles. In a similar experiment (37°C, 2 mM NAC, 15 minutes) on a different batch of vWF carried out under static conditions, the percentage of Cys1458 existing as a free thiol increased from 18% to 32% with NAC treatment.

NAC diminishes the ability of plasma vWF to bind platelets and collagen. In plasma, the platelet-binding activity of vWF correlates with its size — the larger multimers bind platelets better than the smaller ones and are more effective at agglutinating platelets. We examined the ability of NAC-treated plasma to agglutinate fixed platelets in the presence of ristocetin (Figure 4A). In this experiment, the plasma was treated with NAC and the NAC was inactivated before being added to the platelets, so that the effect observed was entirely a consequence of the effect of NAC on vWF. NAC inhibited platelet agglutination in a concentration-dependent manner. Analyzing the data by a piecewise regression model, we found that the minimum concentration of NAC required to reduce

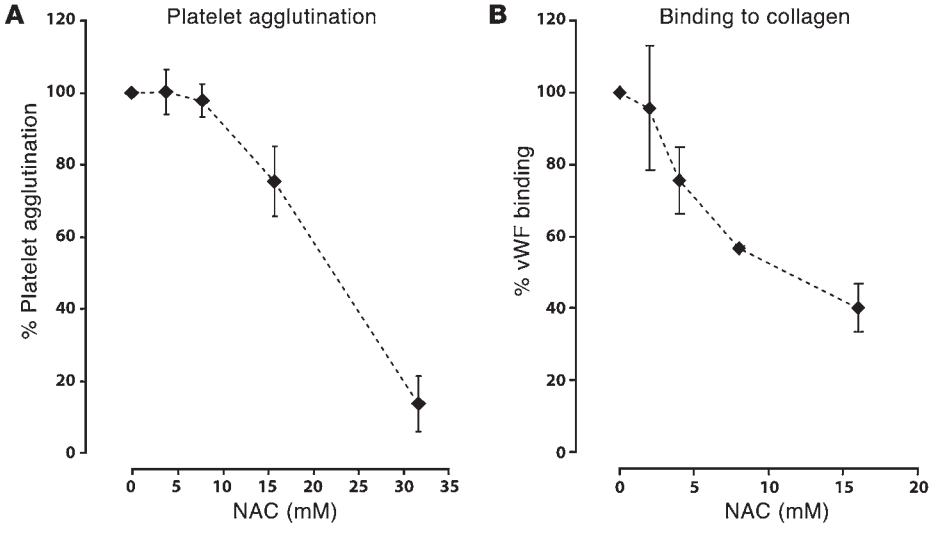

Figure 4
NAC inhibits the ability of vWF to bind platelets and collagen. (**A**) Pooled plasma was incubated with NAC at concentrations of 0, 4, 8, 16, or 32 mM at 37°C for 30 minutes. Residual NAC was then alkylated with NEM. The reaction mixture was used as the source of vWF to agglutinate fixed platelets in the presence of 1 mg/ml of ristocetin. Data represent mean ± SD from 4 independent experiments. (**B**) Purified vWF was incubated with NAC at concentrations of 0, 2, 4, 8, and 16 mM at 37°C for 30 minutes. Residual NAC was then alkylated with NEM. The reaction mixture was added to an ELISA plate coated with collagen, and bound vWF was detected with an HRP-conjugated vWF antibody. Data represent mean ± SD from 3 independent experiments.

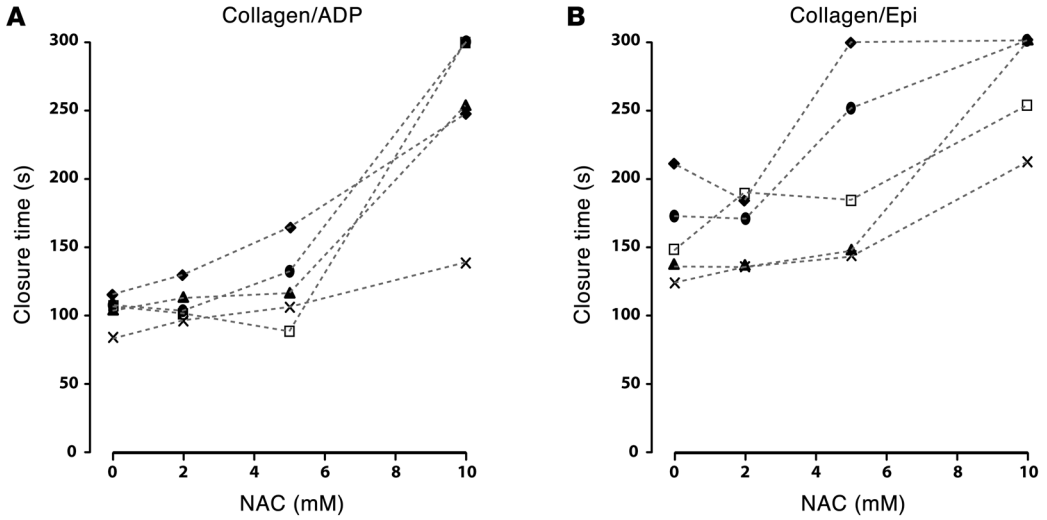

Figure 5

NAC increased the closure time measured by PFA-100. Citrated whole blood was incubated with NAC at the indicated concentrations before being perfused through either a collagen/ADP cartridge (**A**) or a collagen/epinephrine cartridge (**B**) in the PFA-100 device. The closure times increased as the concentration of NAC increased. The machine stopped automatically if closure times were longer than 300 seconds. The mean difference (± SEM) in closure times measured at 10 mM NAC and at 2 mM were significant in both cartridges (**A**: 140 ± 65.6 seconds, $P < 0.005$; **B**: 110 ± 39.7 seconds, $P < 0.005$). There was no difference in closure time measured at 2 mM and 0 mM NAC (**A**: 4.4 ± 9.8 seconds, $P = 0.27$; **B**: 4.9 ± 24.7 seconds, $P = 0.90$). The experiments were repeated on 5 different donors, shown using different symbols. The data were analyzed using Student's *t* test, and the adjusted *P* values are indicated.

platelet agglutination was 10 mM (SEM: ± 1.3 mM). Above this concentration, platelet agglutination decreased by approximately 4% (SEM: ± 0.3%) for each 1 mM increase in NAC concentration.

The capacity of plasma vWF to bind collagen also correlates with multimeric size. NAC inhibited vWF binding to collagen in a concentration-dependent manner (Figure 4B), with the binding at NAC concentrations of 8 and 16 mM being significantly lower than the untreated control samples ($P < 0.05$).

Effect of NAC treatment on PFA-100 closure times. We evaluated the effect of ex vivo NAC treatment on the closure times measured in a PFA-100 (platelet function analyzer), which determines the time required for blood drawn through a cartridge to plug a small hole in a membrane coated with platelet agonists, collagen plus epinephrine, or collagen plus ADP. Formation of the occlusive platelet plug requires adhesion of platelets to the vWF that becomes immobilized on the collagen under high shear stress. Blood was drawn from healthy human volunteers into citrate anticoagulant, and aliquots of the blood were incubated with NAC at various concentrations before loading into the cartridge. Figure 5 depicts the results from the 2 cartridges in blood from 5 volunteers. In all volunteers, the highest concentrations of NAC prolonged the closure times, often to the point that the machine stopped the measurement before closure was achieved. The inhibitory effects of NAC on closure time varied among donors. The closure times at 10 mM NAC were significantly prolonged compared with those measured at 2 mM NAC (Student's *t* test, $P < 0.005$ for both cartridges). There was no difference in closure times between 0 and 2 mM NAC.

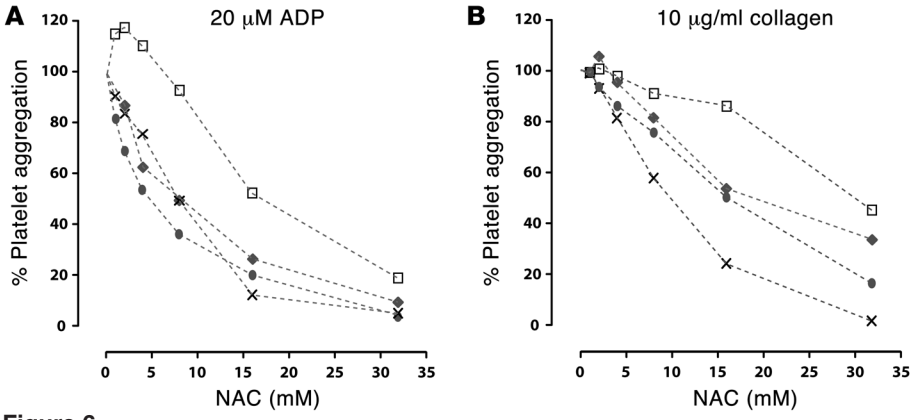

Figure 6

NAC inhibits ADP- and collagen-induced platelet aggregation. Aliquots of citrated platelet-rich plasma were mixed with NAC-containing buffer (NAC concentration: 0, 1, 2, 4, 8, 16, or 32 mM) immediately before addition of agonist. Platelet aggregation was monitored for 5 minutes. Maximum aggregations at the different concentrations of NAC were expressed as a percentage of agonist-induced aggregation in the absence of NAC. NAC inhibited platelet aggregation in a concentration-dependent manner, but the extent of inhibition varied among donors. The inhibitory effects of NAC were observed using 10 and 20 μM ADP or 5 and 10 μg/ml of collagen. Platelet aggregation induced by 20 μM ADP and 10 μg/ml of collagen are shown. Data were obtained from 4 donors, shown using different symbols. Linear regression methods were used to model the dose-response relationships between NAC and platelet aggregation. The equation derived for part **A** was $y = (-18) \log_2 (\times) + 109.8$ (SEM for slope and intercept were ± 1.4 and ± 8.9, respectively); in part **B**, the equation was $y = (-13.4) \log_2 (\times) + 112.2$ (SEM for slope and intercept were ± 1.7 and ± 7.5, respectively). These showed that platelet aggregation induced by either 20 μM ADP or 10 μg/ml collagen decreased as NAC concentration increased.

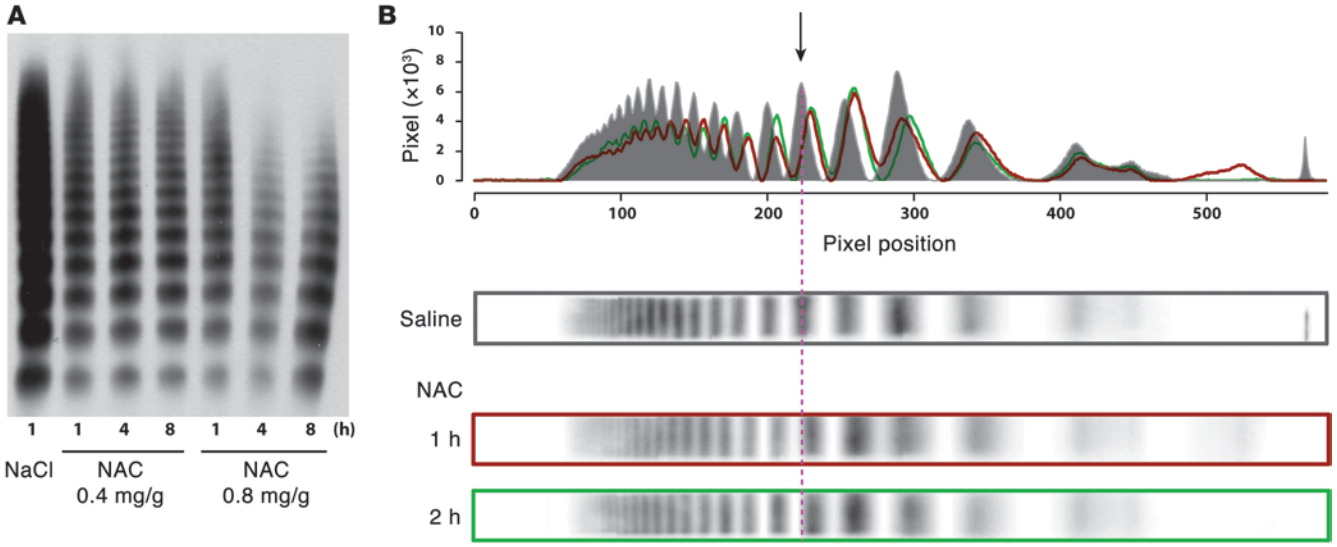

Figure 7
NAC reduced vWF multimers in vivo in C57BL/6 mice. (**A**) Wild-type C57BL/6 mice were injected intravenously with NAC at doses of either 0.4 or 0.8 mg/g. The higher dose had a markedly greater effect on vWF multimer size. The effect was time dependent. (**B**) Densitometry analysis of vWF multimer pattern on a 1.5% agarose gel. Top panel: overlay of densitometry curves of vWF multimers from mice treated with either saline (gray) or with 0.4 mg/g of NAC for 1 hour (red) or 2 hours (green).

Effect of NAC on platelet aggregation induced by ADP and collagen. The results shown in Figure 5 could result from the effects of NAC on vWF or from a combination of effects on platelet function. We tested the effect of NAC on platelet aggregation in response to ADP and collagen. NAC inhibited platelet aggregation induced by 20 μM of ADP or 10 μg/ml of collagen (Figure 6) in a concentration-dependent manner. The extent of inhibition at several NAC concentrations varied among donors, especially in response to collagen. NAC also inhibited platelet aggregation induced by lower concentrations of ADP (10 μM) or collagen (5 μg/ml), with less variation among donors than the higher concentrations (data not shown). Maximal aggregation to 20 μM ADP increased in some donors at the lowest concentrations of NAC; above this concentration, the slope of platelet aggregation versus NAC concentration was virtually identical between donors, as determined using a linear regression model.

Effects of NAC on circulating vWF multimers in wild-type mice. We injected NAC intravenously into wild-type C57BL/6 mice at either 0.4 or 0.8 mg/g and subsequently examined vWF multimers by agarose gel electrophoresis. Both doses reduced vWF multimeric size in a time-dependent manner, with the effect more obvious at the higher dose (Figure 7A). The effect of 0.4 mg/g was difficult to discern on 1% agarose gels (Figure 7A); however, when analyzed on higher resolution 1.5% agarose gels and quantified by scanning densitometry (Figure 7B), the loss of the largest circulating multimers was apparent, as was a downward shift in the molecular mass of each of the multimers, likely reflecting reduction of intrachain disulfide bonds within individual monomers. We observed similar results when the NAC was injected intraperitoneally (not shown). In contrast to the in vitro studies, however, the effect took longer to develop, with the multimers at 4 or 8 hours after the injection being smaller than at 1 hour.

Effect of NAC on ionophore-provoked platelet thrombi viewed by intravital microscopy. We evaluated by intravital microscopy the effect of NAC on induced microvascular thrombosis in both wild-type C57BL/6 and *ADAMTS13*$^{-/-}$ mice. The *ADAMTS13*$^{-/-}$ mice used in our studies had been backcrossed more than 10 times into the C57BL/6 background. Previous studies of *ADAMTS13*$^{-/-}$ mice on a mixed background reported that the size distribution of vWF multimers was no different than in wild-type C57BL/6 mice. We compared multimers in the 2 strains of mice and found that *ADAMTS13*$^{-/-}$ mice

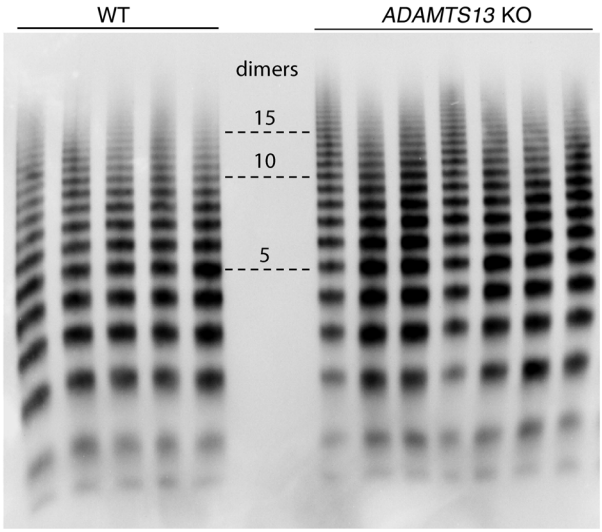

Figure 8
ADAMTS13$^{-/-}$ mice have ULVWF in plasma. vWF multimers in plasma from either wild-type or *ADAMTS13*$^{-/-}$ C57BL/6 mice were separated by electrophoresis on SDS 1% agarose gels and then detected by Western blotting with an HRP-conjugated vWF antibody. Numbers in the center indicate the number of vWF protomers contained in the indicated band. *ADAMTS13*$^{-/-}$ mice displayed a series of high–molecular weight multimers that were larger than the largest seen in wild-type mice.

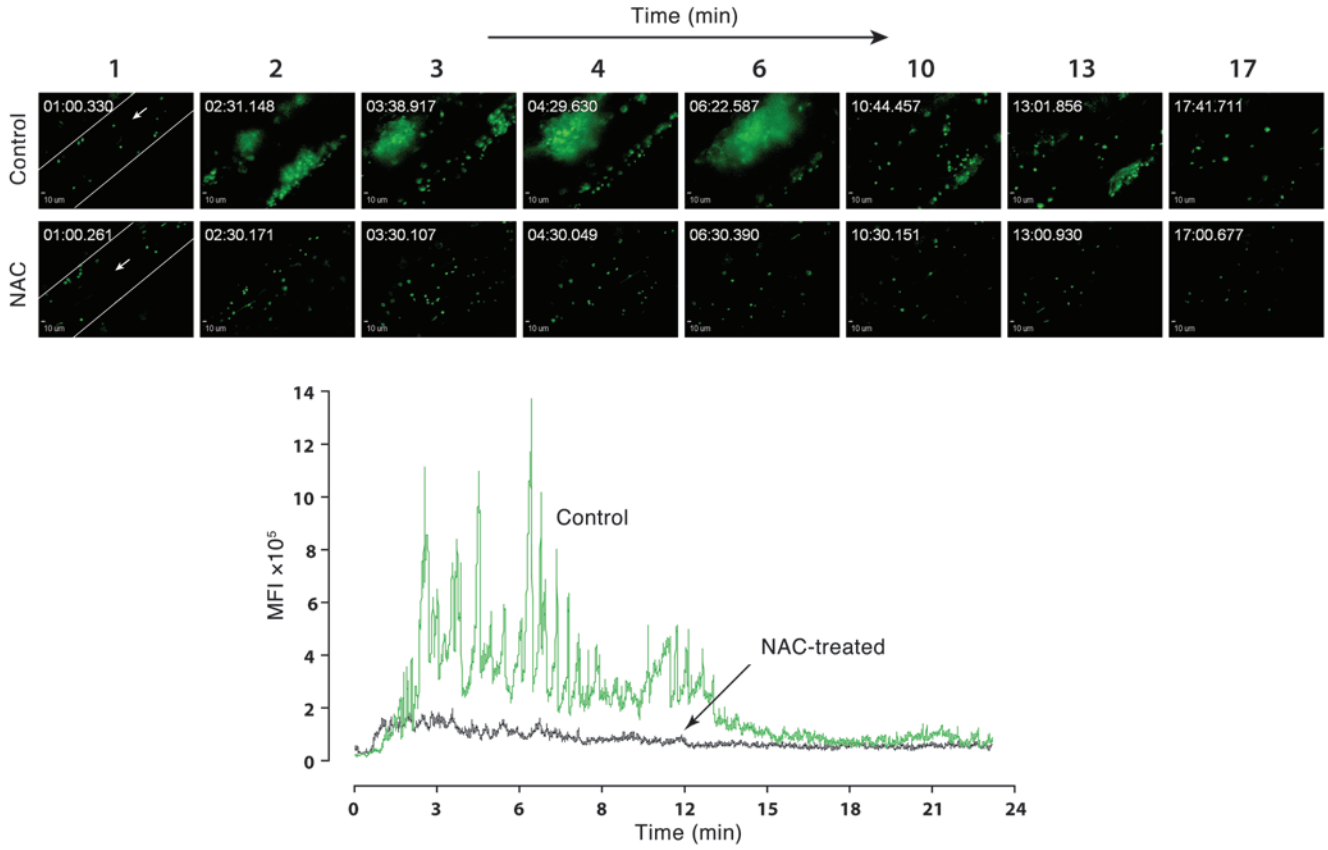

Figure 9
Platelet thrombus accumulation in *ADAMTS13*$^{-/-}$ mice with and without NAC treatment. *ADAMTS13*$^{-/-}$ mice were injected with fluorescently labeled platelets from mice of the same genotype, and their mesenteric vessels were then exposed and treated with calcium ionophore to induce vWF secretion. Platelet accumulation in the vessels was monitored microscopically. Upper panels: sequential images taken at the indicated times after the application of calcium ionophore to *ADAMTS13*$^{-/-}$ mice with or without NAC treatment. Images taken at similar times from the 2 mice are aligned. Original magnification, ×200. Lower panel: MFI of platelet thrombi was quantified on each frame of the recorded movie and plotted against time.

displayed a series of high–molecular weight multimers that were larger than the largest seen in the wild-type C57BL/6 (Figure 8).

The mice were prepared for intravital microscopy and injected with fluorescently labeled platelets that had been isolated from mice of identical genotype. Endothelial cells in mesenteric venules were induced to secrete ULVWF by application of calcium ionophore directly to the vessel, and the accumulation of fluorescent platelets was monitored microscopically. For each mouse, the vessels were monitored and recorded for 3 minutes before the application of ionophore; no platelet adhesion to the vessel wall was detected during this time. Immediately after the application of calcium ionophore, platelets adhered to the vessel wall and could often be seen as strings of single platelets apparently attached to cell-anchored ULVWF strands. Within minutes, multiple platelet thrombi formed and grew to occlude up to 50% of the diameter of the treated vessels in both wild-type and *ADAMTS13*$^{-/-}$ mice (Supplemental Videos 3 and 5). These thrombi were loose and detached easily from the vessel wall. Accumulation of thrombi was monitored over time as a function of the fluorescence intensity in selected vessel segments (Figure 9). In the lower panel of Figure 9, each spike on the plot represents a platelet thrombus as it formed in or flowed through the vessel segment being monitored. In the untreated wild-type mice, thrombi accumulated and repeatedly embolized, with the fluorescence returning to near baseline in a mean time of 6.5 ± 0.5 minutes (Figure 10). This process was markedly prolonged in the *ADAMTS13*$^{-/-}$ mice, the return to baseline requiring an average of 10.4 ±1.2 minutes (Figure 10). In contrast, in the NAC-treated mice, both wild type and *ADAMTS13*$^{-/-}$, the return to baseline was much more rapid (Figure 10 and Supplemental Videos 4 and 6). NAC did not completely prevent platelet thrombus formation in the ionophore-treated vessels, but the thrombi that formed were smaller than those in the untreated mice (Figure 11). These data were quantified from 10 mice in each treatment group.

Effect of NAC on bleeding times in mice. We observed no differences in tail-bleeding times in wild-type C57BL/6 mice treated with either PBS or NAC (0.8 mg/g) by tail-vein injection (Figure 12).

Discussion

Our experiments demonstrate that NAC has many effects that could be of benefit in TTP and other thrombotic disorders involving hyperreactive forms of vWF. These effects included reduction of vWF multimer size, removal of ULVWF strings from the endothelial surface, and marked shortening of the time to reestablish normal blood flow in the microvasculature of ADAMTS13-deficient mice challenged to secrete vWF. Even at concentrations

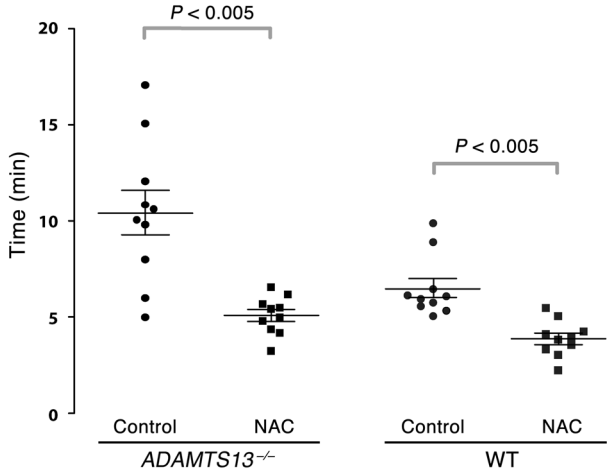

Figure 10
Time to thrombus resolution in calcium ionophore–treated mesenteric venules. Upon calcium ionophore stimulation of the mesenteric venules, platelets immediately began to accumulate on the vessel wall. Adhesion was monitored, and the time required for the fluorescence value to return to baseline was measured. Platelet adhesion persisted longer in mice deficient in *ADAMTS13* than in wild-type mice. NAC treatment in either *ADAMTS13*$^{-/-}$ or wild-type mice significantly shortened the time required for platelet adhesion to return to baseline. The mean (± SEM) values for time to thrombus resolution were as follows. *ADAMTS13*$^{-/-}$: control, 10.4 ± 1.2 minutes; NAC, 5.1 ± 0.3 minutes; wild type: control, 6.5 ± 0.5 minutes; NAC, 3.8 ± 0.3 minutes. 10 mice were examined in each group. The data were analyzed using Student's *t* test, and the adjusted *P* values are indicated.

of NAC with no discernible effect on vWF multimer composition, NAC reduced the disulfide bond encompassing the vWF A1 domain, which is important for vWF's ability to bind platelet GPIb (15). The effect of NAC on vWF's hemostatic potency was demonstrated by its inhibition of platelet agglutination to ristocetin and prolongation of the aperture closure time measured by PFA.

The effects of NAC on vWF in mice were obtained at weight-adjusted doses similar to those used to treat acetaminophen overdose in humans (16, 17). For example, the Danish protocol for treatment of acetaminophen poisoning recommends a total dose of 400 mg/kg delivered as a 150 mg/kg bolus followed by continuous infusion over 36 hours. This dose is identical to the lowest effective dose that was administered to mice as a single bolus in our studies (17).

NAC has other hemostatic effects that could be of benefit in treating thrombosis, including a concentration-dependent inhibition of in vitro platelet aggregation in response to both ADP and collagen. Several studies of the effect of NAC on platelet aggregation have been previously reported (18, 19). For example, NAC prevents NO scavenging by reactive oxygen species in platelets. Some NAC effects may be thiol dependent, as the actions of both ADP and collagen involve thiols. The ADP receptor P_2Y_{12} contains a free thiol that is the target of the platelet function inhibitor clopidogrel (20, 21). Furthermore, optimal collagen-induced platelet aggregation requires the presence of vWF (22).

In reducing vWF disulfide bonds, NAC could have both direct and indirect effects. NAC contains a free thiol, which may reduce the disulfide bonds of vWF directly, as in mucin polymers (14). This is the likely mechanism in our experiments when NAC was added directly to blood or plasma, as the action was rapid and the only cells available to metabolize NAC to other substances were blood cells. In vivo, NAC may also act indirectly after conversion to L-cysteine or by acting as a substrate for augmented synthesis of reduced glutathione (GSH) (23), another bioactive free thiol–containing molecule. It is through this latter mechanism that NAC is effective in treating acetaminophen overdose. Overdose of acetaminophen leads to accumulation of a toxic metabolite, N-acetyl-p-benzo-quinone imine (NAPQI), which is normally only produced in minute amounts (24, 25). NAPQI is detoxified by conjugation with GSH (26), which becomes rapidly depleted in the presence of high acetaminophen concentrations. Unconjugated NAPQI is toxic to the liver (27). NAC works in this case by generating more reduced GSH (28). Thus, in addition to acting directly to reduce ULVWF multimers to smaller and less reactive forms, NAC would also serve to generate reducing equivalents to allow reduction of the vWF in the plasma by other reducing agents, perhaps GSH itself. The existence of such mechanisms to inactivate ULVWF by means other than proteolysis is suggested by the fact that patients with severe congenital *ADAMTS13* deficiency sometimes do not experience acute TTP until the third decade of life (29). Such a reductase would require the continuous provision of reducing equivalents, an action that would be facilitated by NAC. Recent evidence indicates that oxidation of free thiols facilitates vWF self association on surfaces (30); provision of reducing equivalents would tend to prevent this phenomenon.

Our data indicate that NAC may prove useful for treating TTP, as a temporary agent or as supplementary therapy in patients refractory to plasma infusion or exchange. The documented safety profile of NAC makes it a particularly attractive drug for this purpose. NAC has been used in humans for over half a century with few reported adverse effects. Doses as high as 500 mg/kg have been employed to treat acute acetaminophen toxicity (16, 31). NAC has also been evaluated extensively in laboratory animals and found to have an LD_{50} of more than 10 g/kg in both rats and mice when given orally (32), and doses of 1 g/kg have been given daily for up to 2 years in these animals without apparent detrimental effects (32). Caution is warranted, however, because of the recent demonstration that prolonged high-dose NAC therapy or SNO-NAC (the nitric oxide adduct) (10 mg/ml) in the drinking water of mice resulted in pulmonary hypertension (33).

Three studies have addressed the potential adverse hemostatic effects of NAC. Jepsen et al. (34) found that NAC administered intravenously rapidly prolonged the prothrombin time and depressed the activities of clotting factors II, VII, and X. This same group later examined the effect on other hemostatic parameters and concluded that the acute effect was on the vitamin K–dependent factors, with no change noted in vWF antigen levels (17). In a recent report, patients treated with NAC during cardiovascular surgery had increased blood loss compared with untreated patients (35). However, no deaths were reported in the NAC-treated group as compared with 7 deaths in the untreated group ($P = 0.007$), suggesting another beneficial effect of NAC. Our own studies of the effect of NAC administration on the tail-bleeding times in mice surprisingly showed no difference between NAC-treated mice and control mice at either 30 minutes or 8 hours after administration. This result

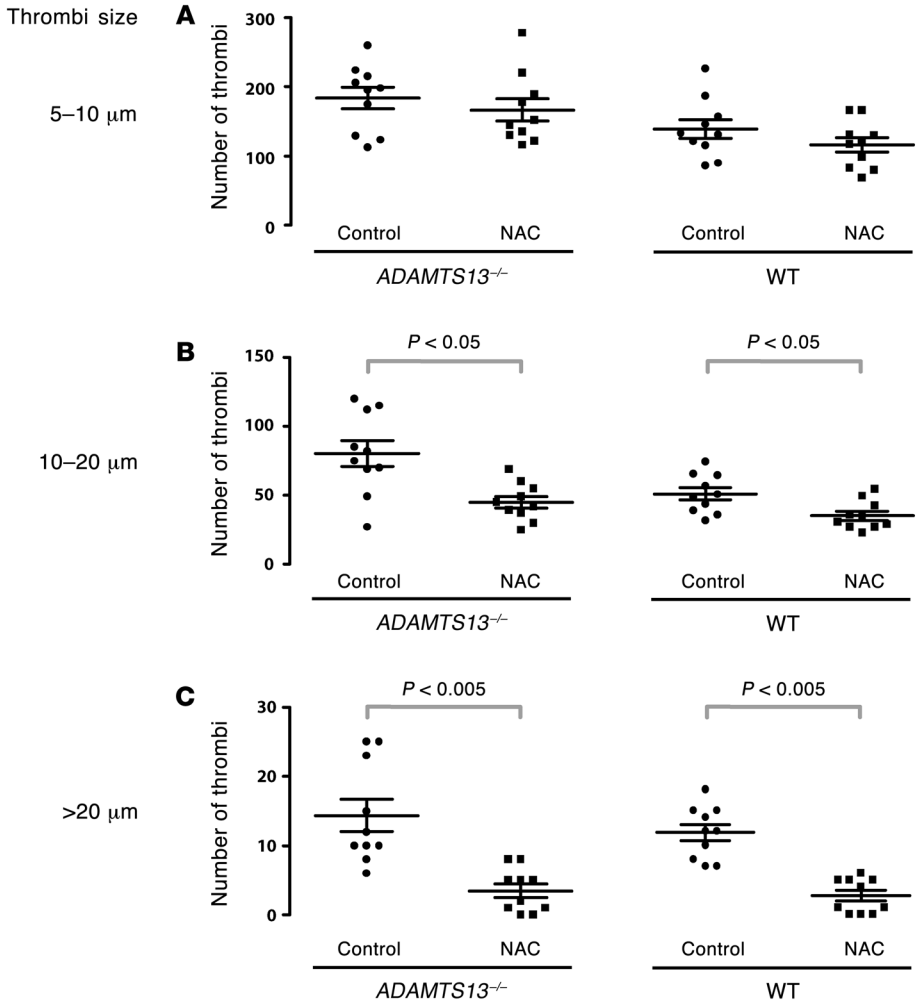

Figure 11
Quantification of platelet thrombi by size. Platelet thrombi in the calcium ionophore–treated vessels were quantified based on diameter: 5–10 μm, 10–20 μm, or larger than 20 μm. Mice of either *ADAMTS13*$^{-/-}$ or wild type treated with NAC had significantly fewer thrombi with diameters of 10–20 μm and larger than 20 μm than the untreated mice (control). The mean (± SEM) numbers of thrombi within the different size ranges were as follows: (**A**) *ADAMTS13*$^{-/-}$: control, 184 ± 15; NAC, 167 ± 16; wild type: control, 138 ± 14; NAC, 115 ± 11. (**B**) *ADAMTS13*$^{-/-}$: control, 80 ± 9, NAC, 45 ± 4; wild type: control, 50 ± 5; NAC, 35 ± 3. (**C**) *ADAMTS13*$^{-/-}$: control, 14.4 ± 2.2; NAC, 3.5 ± 1.0; wild type: control, 11.8 ± 1.2; NAC, 2.7 ± 0.8. 10 mice were examined in each group. The data were analyzed using Student's *t* test, and the adjusted *P* values are indicated.

should be interpreted cautiously, particularly given the many antihemostatic effects of NAC we demonstrated using other tests.

This safety profile makes NAC a potentially useful first-line therapy for TTP when the diagnosis is in doubt or when plasmapheresis is unavailable. For a physician faced with a patient with potential TTP, the diagnosis is rarely clear cut. None of the cardinal signs of TTP are specific for the disease, so they are often ascribed to other syndromes, particularly in the early stages of the clinical course or in patients with concomitant illnesses. Tests to rapidly detect *ADAMTS13* deficiency are not at present routinely available in hospitals, and TTP patients may display near-normal *ADAMTS13* activity (36). The risk of missing the diagnosis of TTP could have disastrous consequences for the patient; yet receiving the presumptive diagnosis of TTP commits that patient to a long and potentially dangerous course of therapy with plasmapheresis. NAC might thus be used to treat TTP while awaiting a definitive diagnosis or availability of plasmapheresis.

Another attractive feature of NAC is its low cost and wide availability. The drug could thus be employed as a temporizing therapy for TTP where plasmapheresis is not readily available. It might also be used in long-term therapy for TTP, especially in those patients with the acquired form of the disorder whose course is self limited when given the appropriate therapy. Clinical trials on healthy individuals and TTP patients will be the next step for determining NAC's utility as an adjunct or first-line therapy of TTP.

If NAC proves useful in TTP, its use could be extended to other syndromes in which hyperactive vWF might also have a role, such as sickle cell anemia (6, 37), myocardial infarction (38), cerebral malaria (39, 40), and stroke (41). We therefore expect that the result of this study may stimulate investigation of NAC as a therapy for several other disorders in which excessive vWF-mediated cell adhesion plays a causative role.

Methods

Materials. The following materials (with their sources indicated in parentheses) were used in this study: NAC (Acetadote; Cumberland Pharmaceuticals Inc.); PFA cartridges and PFA-100 (Dade Behring); calcein AM (Invitrogen); histamine, calcium ionophore, NEM, DTT, and tribromoethanol (Sigma-Aldrich); NEM-d5 (Cambridge Isotope Laboratories); rabbit anti-human vWF antibody (HRP conjugated; Dako North America Inc.); SeaKem gold agarose (Cambrex Bio Science Rockland Inc.); fixed platelets, ADP, collagen (for platelet aggregation), and AggRAM platelet aggregometer (Helena Laboratories Corp.); bovine collagen (for the collagen-binding assay) (MP Biomedicals; LLC); pooled normal plasma in citrate (Precision BioLogic); ristocetin (American Biochemical and Pharmaceutical Ltd.); cone-and-plate viscometer (HAAKE Rheostress 1; Thermo Fisher Scientific); endoproteinase Asp-N (Roche); Finnigan LTQ linear ion trap mass spectrometer (Thermo Electron Corporation).

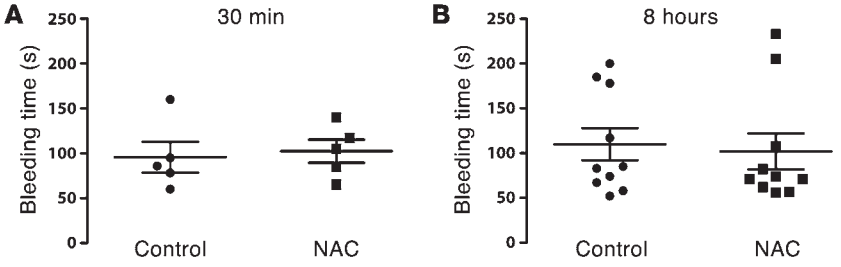

Figure 12
NAC has no effect on bleeding times in mice. Tail-vein bleeding times were examined in 6- to 8-week-old wild-type C57BL/6 mice. Either PBS (control) or NAC (0.8 mg/g) was administered through the tail vein 30 minutes or 8 hours before the bleeding time was determined. Data represent mean ± SEM. The number of mice examined in each group was 5 for **A** and 10 for **B**. No significant differences in bleeding times were observed between treated and untreated mice. The data were analyzed using the Mann-Whitney nonparametric procedure. The adjusted *P* values for the comparisons between control and NAC-treated animals were 0.47 and 0.86, for the 30 minute and 8 hour analyses, respectively.

Blood donors. Blood was drawn from consenting healthy donors under protocols approved by the Institutional Review Boards of Baylor College of Medicine and University of Washington.

Mice. All of the protocols using mice were approved by the Animal Care and Use Committee of Baylor College of Medicine, University of Washington, or St. Michael's Hospital, Toronto. Wild-type C57BL/6 mice were purchased from Jackson Laboratory. Five- to 8-week-old wild-type mice and littermate controls were used for all of the experiments except for those done by intravital microscopy, in which 4-week-old mice were used. ADAMTS13-deficient (*ADAMTS13*$^{-/-}$) mice on a mixed genetic background were a gift from David Motto (University of Iowa, Iowa City, Iowa, USA) and David Ginsburg (University of Michigan, Ann Arbor, Michigan, USA). These mice were subsequently backcrossed for 10 generations onto a C57BL/6 background.

Plasma vWF purification. Plasma vWF was purified from commercial cryoprecipitate prepared at Puget Sound Blood Center. Briefly, cryoprecipitate was first resuspended in citrate buffer and then 2 M glycine was added to precipitate the bulk of the fibrinogen. After removing the fibrinogen, vWF was precipitated by adding 1.5 M NaCl. The vWF precipitate was then resuspended in 25 mM Hepes buffer, pH 6.8, before further purification on a size-exclusion column. Fractions of the column flow-though were collected, and the antigen concentration was measured by UV absorption at 280 nm. The relevant fractions were pooled before use.

HUVECs. Endothelial cells from human umbilical cord vein were isolated as previously described (42).

NAC treatment of vWF under static conditions. Purified vWF was treated with NAC at final concentrations ranging from 0 to 16 mM at 37°C for 30 minutes. Pooled normal human plasma in citrate was incubated with NAC at concentrations of 0, 4, 8, 16, or 32 mM at 37°C for 1 hour. The reactions were stopped by adding NEM to alkylate the residual NAC. In preparation for electrophoresis, the samples were mixed with equal volumes of gel loading buffer (50 mM Tris, 6 M urea, 10 mM EDTA, 2% SDS, and 0.03% bromphenol blue, pH 6.8), and then heated at 60°C for 20 minutes. The vWF multimer pattern was examined by SDS–1% agarose gel electrophoresis as described previously (4).

NAC treatment of ULVWF under flow. These experiments took advantage of our earlier observation that when endothelial cells are stimulated with histamine and subsequently perfused with a plasma-free suspension of platelets, the platelets form long beads-on-a-string structures on the endothelial surface that represent cell-attached ULVWF that has been decorated with the platelets (43). In this assay, HUVECs grown on a 35-mm culture dish were first stimulated with 100 μM histamine at 37°C for 2 minutes and the dish was then assembled as the bottom of a parallel-plate flow chamber. In the experiments represented by Supplemental Videos 1 and 2, the chamber was then perfused for the indicated times with buffer and NAC (40 mM), respectively. In the experiments depicted in Figure 2, washed platelets suspended in Tyrode's buffer were perfused at 2.5 dynes/cm^2 over the histamine-stimulated HUVECs for 2 minutes; then 40 mM NAC was perfused for 20–30 minutes, Tris buffer (Ca^{2+}/Mg^{2+}-free) was perfused for 2 minutes, and the chamber was perfused again with fresh, washed platelets for 2 minutes. The number of ULVWF-platelet strings was quantified in 20 continuous microscopic fields (×400 magnification) as previously described (43).

Quantification of free thiols in NAC- or DTT-treated vWF by mass spectrometry. Purified plasma vWF in 25 mM HEPES buffer was sheared on a cone-and-plate viscometer at 37°C, 10,000 s^{-1} for 15 minutes without reducing agent (0 mM) or in the presence of DTT (100 μM or 1 mM) or NAC (2 mM). The samples were then mixed immediately with NEM to alkylate the residual NAC or DTT to prevent further disulfide bond shuffling. Free thiols in the treated vWF were labeled with 80 mM NEM under denaturing conditions (6 M guanidine HCl) at 37°C for 1 hour in Tris buffer, pH 7.0. The alkylated proteins were separated from excess NEM by precipitation with 10–20 volumes of cold ethanol at –20°C and then resuspended in Tris buffer (pH 7.4) containing 6 M guanidine HCl. The cysteines involved in disulfide bonds in the samples were labeled with 25 mM NEM-d5 in the presence of 10 mM DTT at 60°C. After another ethanol precipitation to remove excess NEM-d5, the recovered protein was digested by endoproteinase Asp-N at a ratio of 50:1 (w/w) protein/Asp-N in Tris buffer (pH 8.0) containing 1 mM $MgCl_2$ and 0.1% RapiGest. Digestion was halted by acidification (pH 2–3) with 10% (v/v) trifluoroacetic acid. The peptides were analyzed by nanospray-liquid chromatography–tandem mass spectrometry (Nano-LC-MS/MS) in the positive ion mode with a Finnigan LTQ linear ion trap mass spectrometer coupled to a Paradigm MS4 (Michrom BioResources Inc). Peptides were separated on a Magic C18 AQ column (150 × 0.15 mm, 5 μm 200Å, Michrom BioResources Inc) using solvent A (0.1% formic acid, 5% CH_3CN in water) and solvent B (0.1% formic acid in 90% CH_3CN). Peptides were eluted using a linear gradient of 5%–35% solvent B over 180 minutes. The spray voltage was 1.8 kV, and the temperature of the heated capillary was 200°C. NEM- or NEM-d5–labeled peptide ions were detected by selected reaction monitoring. The percentage of free thiols was determined by dividing the area of the peak from the NEM-alkylated peptide by the sum of peak areas from the NEM- and NEM-d5–alkylated peptides.

Ristocetin-induced platelet agglutination. Aliquots of pooled normal plasma in citrate were incubated with either HEPES buffer (final HEPES concentration 10 mM, pH 7.4) or NAC at concentrations of 4, 8, 16, or 32 mM at 37°C for 30 minutes. Residual NAC was alkylated by adding NEM to a final concentration of 64 mM. The reaction mixture was used as the source of vWF to agglutinate fixed platelets in the presence of 1 mg/ml of ristocetin. The percentage of aggregation obtained using NAC-treated plasma was normalized to that from buffered-treated plasma, which was considered 100%. Mean values from 4 independent experiments are shown.

vWF binding to collagen. The collagen-binding assay was performed as described by Favaloro et al. (44). Briefly, aliquots of purified vWF were first incubated with either PBS or NAC at concentrations of 2, 4, 8, and 16 mM at 37°C for 30 minutes. Residual NAC was alkylated with NEM. The reaction mixture was added to an ELISA plate coated with bovine

collagen (95% type I and 5% type III). The bound vWF was detected by HRP-conjugated vWF antibody. The binding of NAC-treated vWF was normalized to untreated vWF, and mean values from 3 independent experiments were shown.

PFA-100 platelet function analyzer. Cartridges used contained membranes coated either with collagen/adenosine diphosphate (ADP) or collagen/epinephrine. Aliquots of blood drawn from healthy human volunteers into citrate anticoagulant (3.8% sodium citrate, w/v) were treated with NAC at various concentrations at room temperature for 5 minutes before being loaded onto the collagen/Epi cartridge, or for 15 minutes before being loaded onto the collagen/ADP cartridge. The time required for occlusion of the aperture was recorded by the machine. Untreated blood from the same donor served as a control for the NAC-treated blood.

NAC treatment of wild-type C57BL/6 mice. Six- to 8-week-old wild-type C57BL/6 mice and littermate controls were used in these experiments. Saline or NAC solution was injected through the tail vein. At 1, 2, 4, or 8 hours after NAC injection, the mice were anesthetized and blood was drawn into 1.5% EDTA solution (pH 8) from the inferior vena cava in a terminal phlebotomy. Platelet-poor plasma was isolated by centrifugation at 500 *g* for 15 minutes. The vWF multimer pattern in the plasma was then examined by agarose gel electrophoresis. Samples of different time points represent individual mice.

Densitometric analysis of vWF multimers. Plasma vWF from either control or NAC-treated mice was separated on a 1.5% agarose gel by electrophoresis. vWF was detected by HRP-conjugated vWF antibody in Western blots, and the chemiluminescent signals were captured by CCD camera (ImageQuant 350; GE Healthcare Life Sciences). The digital imagines were analyzed by ImageQuant TL software, which automatically detected vWF "ladders" based on the signal intensity.

Intravital microscopy. We studied 4-week-old male mice of either wild-type C57BL/6 or congenic *ADAMTS13*$^{-/-}$ genotypes. The mice were prepared as described previously (45–47). Briefly, blood was collected into ACD (1:10) from the retro-orbital plexus of mice matching the genotype of the experimental mice. Platelet-rich plasma was prepared by centrifugation. Platelets were separated from plasma by gel filtration and labeled with 1 mg/ml of calcein AM at room temperature for 20 minutes and then injected into the experimental mouse (1.25×10^6 platelets/g) through the tail vein. The mice were then anesthetized and the mesentery was externalized. In each mouse, a single mesenteric venule of 120 to 150 μm diameter was chosen and treated topically with 10 μl of 10 μM calcium ionophore to induce Weibel-Palade body secretion. NAC (0.4 mg/g) was injected into the tail vein 5–10 minutes before calcium ionophore stimulation. Images of thrombus formation and dissolution visualized through a fluorescence microscope (Zeiss Axiovert 135; Zeiss Oberkochen) were recorded for 20 minutes using a videocassette recorder. We quantified the number of thrombi formed after calcium ionophore stimulation and the time required for platelet adhesion to the vessel wall to return to baseline.

Fluorescence in the vessels arising from platelet thrombi, individual platelets attached to the vessel wall, or platelets embolizing through the field of view was recorded with a digital camera (CoolSNAP) and analyzed using SlideBook software. We monitored 3 mice per group.

Bleeding time. Wild-type C57BL/6 mice (6–8 weeks old) were injected with either PBS or NAC (0.8 mg/g) intravenously via the tail vein 30 minutes or 8 hours before the bleeding time was assessed. Mice were anesthetized with 2.5% tribromoethanol (0.015 ml/g) and maintained at 37°C on a heating pad during the experiment. The tip of the tail (3 mm) was cut off with a sharp scalpel, and the tail was immediately placed into warm saline of 37°C. The bleeding time was the period from the moment blood began emerging from the cut until the moment bleeding ceased.

Statistics. Independent or paired *t* tests were used to compare group means for data presented in Figure 2, Figure 4B, Figure 5, Figure 10, and Figure 11. Differences in bleeding times between NAC and control mice (Figure 12) were analyzed using the Mann-Whitney nonparametric procedure. A piece-wise regression method was used to model dose-response relationships between NAC concentration and platelet agglutination for data presented in Figure 4A. Linear regression methods were used to model dose-response relationships between NAC and platelet aggregation for data presented in Figure 6. $P \leq 0.05$ was considered significant. *P* values have been adjusted when making multiple comparisons using the Šidák or Bonferroni corrections as appropriate.

Acknowledgments

The authors thank Jennie Le and Yi Wang for assistance with the experiments and Doug Bolgiano for assistance with statistical analysis. This work was supported by NIH grants P50 HL65967 and RO1 HL091153, American Heart Association grant 0630180N, Bayer Hemophilia Awards, the Heart and Stroke Foundation of Canada (Ontario), the Canada Foundation of Innovation, institutional funds from the Puget Sound Blood Center, and the Mary R. Gibson Foundation.

Received for publication September 3, 2009, and accepted in revised form November 17, 2010.

Address correspondence to: José A. López, Research Division, Puget Sound Blood Center, 921 Terry Ave., Seattle, Washington 98104, USA. Phone: 206.398.5930; Fax: 206.587.6056; E-mail: josel@psbcresearch.org.

1. Tsai HM. Current concepts in thrombotic thrombocytopenic purpura. *Annu Rev Med*. 2006;57:419–436.
2. Lian EC, Harkness DR, Byrnes JJ, Wallach H, Nunez R. Presence of a platelet aggregating factor in the plasma of patients with thrombotic thrombocytopenic purpura (TTP) and its inhibition by normal plasma. *Blood*. 1979;53(2):333–338.
3. Moake JL, et al. Unusually large plasma factor VIII: von Willebrand factor multimers in chronic relapsing thrombotic thrombocytopenic purpura. *N Engl J Med*. 1982;307(23):1432–1435.
4. Moake JL, Turner NA, Stathopoulos NA, Nolasco LH, Hellums JD. Involvement of large plasma von Willebrand factor (vWF) multimers and unusually large vWF forms derived from endothelial cells in shear stress-induced platelet aggregation. *J Clin Invest*. 1986;78(6):1456–1461.
5. Li F, Moake JL, McIntire LV. Characterization of von Willebrand factor interaction with collagens in real time using surface plasmon resonance. *Ann Biomed Eng*. 2002;30(9):1107–1116.
6. Wick TM, Moake JL, Udden MM, Eskin SG, Sears DA, McIntire LV. Unusually large von Willebrand factor multimers increase adhesion of sickle erythrocytes to human endothelial cells under controlled flow. *J Clin Invest*. 1987;80(3):905–910.
7. Furlan M, Robles R, Lamie B. Partial purification and characterization of a protease from human plasma cleaving von Willebrand factor to fragments produced by in vivo proteolysis. *Blood*. 1996;87(10):4223–4234.
8. Tsai HM. Physiologic cleavage of von Willebrand factor by a plasma protease is dependent on its conformation and requires calcium ion. *Blood*. 1996;87(10):4235–4244.
9. Darabi K, Berg AH. Rituximab can be combined with daily plasma exchange to achieve effective B-cell depletion and clinical improvement in acute autoimmune TTP. *Am J Clin Pathol*. 2006;125(4):592–597.
10. Sadler JE. Biochemistry and genetics of von Willebrand factor. *Annu Rev Biochem*. 1998;67:395–424.
11. Vischer UM, Wagner DD. von Willebrand factor proteolytic processing and multimerization precede the formation of Weibel-Palade bodies. *Blood*. 1994;83(12):3536–3544.
12. Perez-Vilar J, Hill RL. The structure and assembly of secreted mucins. *J Biol Chem*. 1999; 274(45):31751–31754.
13. Kelly GS. Clinical applications of N-acetylcysteine. *Altern Med Rev*. 1998;3(2):114–127.
14. Sheffner AL, Medler EM, Jacobs LW, Sarett HP. The in vitro reduction in viscosity of human tracheobronchial secretions by acetylcysteine. *Am Rev Respir Dis*. 1964;90:721–729.
15. Cruz MA, Handin RI, Wise RJ. The interaction of the von Willebrand factor-A1 domain with platelet glycoprotein Ib/IX. The role of glycosylation and disulfide bonding in a monomeric recombinant A1 domain protein. *J Biol Chem*. 1993;268(28):21238–21245.
16. Heard KJ. Acetylcysteine for acetaminophen poisoning. *N Engl J Med*. 2008;359(3):285–292.

17. Knudsen TT, et al. Effect of intravenous N-acetylcysteine infusion on haemostatic parameters in healthy subjects. *Gut*. 2005;54(4):515–521.
18. Loscalzo J. N-Acetylcysteine potentiates inhibition of platelet aggregation by nitroglycerin. *J Clin Invest*. 1985;76(2):703–708.
19. Anfossi G, Russo I, Massucco P, Mattiello L, Cavalot F, Trovati M. N-acetyl-L-cysteine exerts direct anti-aggregating effect on human platelets. *Eur J Clin Invest*. 2001;31(5):452–461.
20. Ding Z, Kim S, Dorsam RT, Jin J, Kunapuli SP. Inactivation of the human P2Y12 receptor by thiol reagents requires interaction with both extracellular cysteine residues, Cys17 and Cys270. *Blood*. 2003;101(10):3908–3914.
21. Savi P, et al. The active metabolite of Clopidogrel disrupts P2Y12 receptor oligomers and partitions them out of lipid rafts. *Proc Natl Acad Sci U S A*. 2006;103(29):11069–11074.
22. Bernardo A, et al. Von Willebrand factor present in fibrillar collagen enhances platelet adhesion to collagen and collagen-induced platelet aggregation. *J Thromb Haemost*. 2004;2(4):660–669.
23. Corcoran GB, Wong BK. Role of GSH in prevention of acetaminophen-induced hepatotoxicity by N-acetyl-L-cysteine in vivo: studies with N-acetyl-D-cysteine in mice. *J Pharmacol Exp Ther*. 1986;238(1):54–61.
24. Jollow DJ, Thorgeirsson SS, Potter WZ, Hashimoto M, Mitchell JR. Acetaminophen–induced hepatic necrosis. VI. Metabolic disposition of toxic and nontoxic doses of acetaminophen. *Pharmacology*. 1974;12(4–5):251–271.
25. Jollow DJ, Mitchell JR, Potter WZ, Davis DC, Gillette JR, Brodie BB. Acetaminophen-induced hepatic necrosis. II. Role of covalent binding in vivo. *J Pharmacol Exp Ther*. 1973;187(1):195–202.
26. Mitchell JR, Jollow DJ, Potter WZ, Gillette JR, Brodie BB. Acetaminophen-induced hepatic necrosis. IV. Protective role of glutathione. *J Pharmacol Exp Ther*. 1973;187(1):211–217.
27. Potter WZ, Thorgeirsson SS, Jollow DJ, Mitchell JR. Acetaminophen-induced hepatic necrosis. V. Correlation of hepatic necrosis, covalent binding and glutathione depletion in hamsters. *Pharmacology*. 1974;12(3):129–143.
28. Lauterburg BH, Corcoran GB, Mitchell JR. Mechanism of action of N-acetylcysteine in the protection against the hepatotoxicity of acetaminophen in rats in vivo. *J Clin Invest*. 1983;71(4):980–991.
29. Furlan M, Lammle B. Aetiology and pathogenesis of thrombotic thrombocytopenic purpura and haemolytic uraemic syndrome: the role of von Willebrand factor-cleaving protease. *Best Pract Res Clin Haematol*. 2001;14(2):437–454.
30. Li Y, et al. Covalent regulation of ULVWF string formation and elongation on endothelial cells under flow conditions. *J Thromb Haemost*. 2008; 6(7):1135–1143.
31. Miller LF, Rumack BH. Clinical safety of high oral doses of acetylcysteine. *Semin Oncol*. 1983; 10(1 suppl 1):76–85.
32. Johnston RE, Hawkins HC, Weikel JH Jr. The toxicity of N-acetylcysteine in laboratory animals. *Semin Oncol*. 1983;10(1 suppl 1):17–24.
33. Palmer LA, et al. S-nitrosothiols signal hypoxia-mimetic vascular pathology. *J Clin Invest*. 2007; 117(9):2592–2601.
34. Jepsen S, Hansen AB. The influence of N-acetylcysteine on the measurement of prothrombin time and activated partial thromboplastin time in healthy subjects. *Scand J Clin Lab Invest*. 1994;54(7):543–547.
35. Wijeysundera DN, et al. N-acetylcysteine is associated with increased blood loss and blood product utilization during cardiac surgery. *Crit Care Med*. 2009;37(6):1929–1934.
36. Vesely SK, et al. *ADAMTS13* activity in thrombotic thrombocytopenic purpura-hemolytic uremic syndrome: relation to presenting features and clinical outcomes in a prospective cohort of 142 patients. *Blood*. 2003;102(1):60–68.
37. Kaul DK, Nagel RL, Chen D, Tsai HM. Sickle erythrocyte-endothelial interactions in microcirculation: the role of von Willebrand factor and implications for vasoocclusion. *Blood*. 1993;81(9):2429–2438.
38. Spiel AO, Gilbert JC, Jilma B. von Willebrand factor in cardiovascular disease: focus on acute coronary syndromes. *Circulation*. 2008;117(11):1449–1459.
39. Bridges DJ, et al. Rapid activation of endothelial cells enables Plasmodium falciparum adhesion to platelet-decorated von Willebrand factor strings. *Blood*. 2010;115(7):1472–1474.
40. Lopez JA. Malignant malaria and microangiopathies: merging mechanisms. *Blood*. 2010; 115(7):1317–1318.
41. Conway DS, Pearce LA, Chin BS, Hart RG, Lip GY. Prognostic value of plasma von Willebrand factor and soluble P-selectin as indices of endothelial damage and platelet activation in 994 patients with nonvalvular atrial fibrillation. *Circulation*. 2003;107(25):3141–3145.
42. Nolasco LH, et al. Hemolytic uremic syndrome-associated Shiga toxins promote endothelial-cell secretion and impair *ADAMTS13* cleavage of unusually large von Willebrand factor multimers. *Blood*. 2005;106(13):4199–4209.
43. Dong JF, et al. ADAMTS-13 rapidly cleaves newly secreted ultralarge von Willebrand factor multimers on the endothelial surface under flowing conditions. *Blood*. 2002;100(12):4033–4039.
44. Favaloro EJ. Collagen binding assay for von Willebrand factor (VWF:CBA): detection of von Willebrands Disease (VWD), and discrimination of VWD subtypes, depends on collagen source. *Thromb Haemost*. 2000;83(1):127–135.
45. Ni H, et al. Persistence of platelet thrombus formation in arterioles of mice lacking both von Willebrand factor and fibrinogen. *J Clin Invest*. 2000; 106(3):385–392.
46. Reheman A, et al. Vitronectin stabilizes thrombi and vessel occlusion but plays a dual role in platelet aggregation. *J Thromb Haemost*. 2005;3(5):875–883.
47. Reheman A, et al. Plasma fibronectin depletion enhances platelet aggregation and thrombus formation in mice lacking fibrinogen and von Willebrand factor. *Blood*. 2009;113(8):1809–1817.